



**HAL**  
open science

## Morphology and Ecology of Two New Amoebae, Isolated From a Thalassohaline Lake, Dziani Dzaha

Willy Aucher, Vincent Delafont, Elodie Ponlaitiac, Aurélien Alafaci, Hélène Agogué, Christophe Leboulanger, Marc Bouvy, Yann Héchard

### ► To cite this version:

Willy Aucher, Vincent Delafont, Elodie Ponlaitiac, Aurélien Alafaci, Hélène Agogué, et al.. Morphology and Ecology of Two New Amoebae, Isolated From a Thalassohaline Lake, Dziani Dzaha. *Protist*, 2020, 171 (6), pp.125770. 10.1016/j.protis.2020.125770 . hal-03024315

**HAL Id: hal-03024315**

**<https://hal.science/hal-03024315>**

Submitted on 14 Dec 2020

**HAL** is a multi-disciplinary open access archive for the deposit and dissemination of scientific research documents, whether they are published or not. The documents may come from teaching and research institutions in France or abroad, or from public or private research centers.

L'archive ouverte pluridisciplinaire **HAL**, est destinée au dépôt et à la diffusion de documents scientifiques de niveau recherche, publiés ou non, émanant des établissements d'enseignement et de recherche français ou étrangers, des laboratoires publics ou privés.

1 **Morphology and ecology of two new amoebae, isolated from a**  
2 **thalassohaline lake, Dziani Dzaha.**

3 Willy Aucher<sup>a</sup>, Vincent Delafont<sup>a</sup>, Elodie Ponlaitiac<sup>a</sup>, Aurélien Alafaci<sup>a</sup>, Hélène Agogué<sup>b</sup>,  
4 Christophe Leboulanger<sup>c</sup>, Marc Bouvy<sup>c</sup> and Yann Héchard<sup>a</sup>

5 <sup>a</sup> Laboratoire Ecologie et Biologie des Interactions (EBI), Equipe Microbiologie de l'Eau,  
6 Université de Poitiers, UMR CNRS 7267, Poitiers, France.

7 <sup>b</sup> Littoral Environnement et Sociétés (LIENSs), UMR 7266 CNRS – La Rochelle Université,  
8 2 rue Olympe des Gouges, 17 000 La Rochelle, France

9 <sup>c</sup> : Unité MARBEC (Marine Biodiversity, Exploitation and Conservation), Université de  
10 Montpellier, IRD, Ifremer, CNRS ; Place Eugène Bataillon, case 063, 34095, Montpellier  
11 cedex 5, France.

12 Corresponding author:

13 [Yann.hechard@univ-poitiers.fr](mailto:Yann.hechard@univ-poitiers.fr)

## 14 **Abstract**

15 Dziani Dzaha is a hypersaline lake (Mayotte island), whose microbial community is dominated  
16 by photosynthetic microorganisms. Here, we describe two new free-living heteroloboseans.  
17 One belonging to the *Pharyngomonas* genus and the other, whose 18S rRNA gene sequence  
18 shares only 85% homology to its closest relatives *Euplaesiobystra hypersalinica*, was proposed  
19 as a new species of this genus being called *Euplaesiobystra dzianiensis*. Both strains were salt  
20 tolerant to 75‰ and grew between 25 and 37°C. Their distribution patterns varied seasonally  
21 and depended also on depth. Noticeably, both free-living amoebae isolates were able to graze  
22 on *Arthrospira* filaments, which are found within the same water layer. In conclusion, we  
23 document for the first time the presence and ecology of free-living amoebae in the  
24 thalassohaline lake Dziani Dzaha, and describe a new species of the *Euplaesiobystra* genus.

25 **Key words: Arthrospira, grazing, halotolerant, Heterolobosea, thalassohaline, water.**

## 26 **Introduction**

27 Thalassohaline ecosystems are hypersaline lacustrine environments whose water is of marine  
28 origin, unlike soda lakes which are filled with water originating from surrounding watersheds  
29 and concentrated by solar evaporation, thus qualifying as athalassohaline. The lake Dziani  
30 Dzaha, located in a tropical area (Mayotte island, Southwestern Indian Ocean) is a *bona fide*  
31 thalassohaline lake (Leboulanger et al., 2017) formed in a crater likely resulting from an  
32 eruptive event that occurred during the late Pleistocene/early Miocene era (Nougier et al., 1986;  
33 Zinke et al., 2003). The lake reaches a maximum depth of 18 m, presents a permanent anoxic  
34 zone below 1.5 m and a periodic chemocline around 14 m. During the rainy period (December-  
35 April), the upper layer is diluted creating a seasonal pycnocline, while during the dry period  
36 (June-November) salinity is constant over depth. Lake water is warm (29-35°C) over the whole  
37 year and depth; pH is alkaline, classically between 9 and 9.5 depending on the season. The lake  
38 Dziani Dzaha microbial planktonic community has recently been described via a  
39 metabarcoding approach (Hugoni et al., 2018). Bacterial and archaeal diversity was influenced  
40 mainly by the sampling depth, whereas dry and rainy seasons alternations drove changes in  
41 vertical segregation of microorganisms. Photosynthetic microorganisms were the most  
42 abundant and were typically present in surface layers, while chemotrophic taxa and  
43 methanogenic archaea were more abundant in the deeper layers. Eukaryotic diversity was  
44 highly influenced by the season, and to a lower extent by the depth. Overall, the diversity was  
45 dominated by photosynthetic organisms: the cyanobacteria *Arthrospira fusiformis* representing

46 on average 48% of the total sequences in most layers, especially during the dry season, and the  
47 eukaryotic chlorophyte *Picocystis salinarum* representing 15% of the total sequences, which  
48 was by far the most abundant eukaryotic taxon. Apart from *Picocystis*, various eukaryotes were  
49 detected belonging to Fungi, Stramenopiles, and ciliates. Noticeably, no amoebae have been  
50 detected, although such microorganisms have been found in hypersaline environments before  
51 (Park and Simpson, 2015).

52 Free-living amoebae (FLA) are chemotrophic protists found in various environments, such as  
53 water and soil. They belong mainly to the Amoebozoa, Excavata (Heterolobosea) and Rhizaria  
54 groups (Samba-Louaka et al., 2019). Heterolobosean were previously described in hypersaline  
55 environments, such as soda lakes and solar salterns (Finlay et al., 1987; Park et al., 2009; Park  
56 and Simpson, 2011; Plotnikov et al., 2015). Heterolobosea have a diversity of life stages: some  
57 genera are known as pure flagellates, such as *Percolomonas* (Nikolaev et al., 2004),  
58 *Pleurostomum* (Park et al., 2007) and *Aurem* (Jhin and Park, 2019), while others, such as  
59 *Naegleria* (De Jonckheere, 2014), *Tetramitus* (Baumgartner et al., 2009), *Tulamoeba* (Park et  
60 al., 2009), *Euplaesiobystra* (Park et al., 2009) and *Pharyngomonas* (Harding et al., 2013),  
61 switch from an amoeba stage to a flagellate one, which make them refer to as  
62 amoeboflagellates. Heterolobosea possess characteristic eruptive cytoplasmic flow that allow  
63 them to move and feed. They mainly graze on bacteria by phagocytosis (Pánek et al., 2017).  
64 Many of them are also able to differentiate into a cyst (dormant stage).

65 The aim of our study was to assess the presence of amoebae in the lake Dziani Dzaha by a  
66 culture-based approach. We hereby characterize two new heterolobosean isolates affiliated to  
67 *Pharyngomonas* and *Euplaesiobystra* genera. Their presence was researched throughout  
68 different seasons and along the water column. Experiments were performed to explore whether  
69 the isolated amoebae could graze filamentous cyanobacteria, which constitutes the highest  
70 biomass in the lake Dziani Dzaha.

## 71 **Results**

72 *Pharyngomonas* sp. DD1

### 73 **Morphology and Ultrastructure**

74 Light microscopic observations of *Pharyngomonas* sp. DD1 showed a typical morphology for  
75 this genus, most notably root-like extensions (Fig. 1). *Pharyngomonas* sp. DD1 trophozoites  
76 ( $27 \pm 12.9 \mu\text{m}$  long (between 14 and 64  $\mu\text{m}$ ),  $12 \pm 2.5 \mu\text{m}$  wide (between 7.5 and 19.4  $\mu\text{m}$ ))  
77 presented a variety of shapes, including elongated forms that are present in older cultures, as



78 previously observed in other *Pharyngomonas* strains (Harding et al., 2013; Plotnikov et al.,  
79 2015). It can switch from long crenulated forms (Fig. 1A and 1D) to flabellate shapes or to  
80 more ovoid ones (Fig. 1B and 1C). When cells are elongated, they can deploy finger-like  
81 pseudopodia as well as very long root-like extensions (which can represent half to two-thirds  
82 of the cell length), these being more visible before encystment. This FLA isolate formed round  
83 or ovoid-shaped cysts ( $10.5 \pm 1 \mu\text{m}$  diameter) that appeared doubled-layered. The ectocyst  
84 thickness is quite variable, the cyst being surrounded by "bead-like" structures, or crypts as  
85 previously referred to (Park and Simpson, 2016). No ostiole could be clearly distinguished.  
86 Encystment of a trophozoite culture is very synchronous for this strain and takes place in less  
87 than 24 hours, as soon as bacterial substrate has been depleted. Despite numerous observations,  
88 we were unable to see a flagellate form, which was described for all other *Pharyngomonas*  
89 strains except *P. turkanaensis* (Park and Simpson, 2016).

90 Transmission electron microscopy was performed to describe the ultrastructure of this isolate  
91 (Fig. 2). The nucleus was clearly visible, and the nucleolus can be distinguished (Fig. 2B, 2C  
92 and 2D). Numerous elongated mitochondria were present in the whole cytoplasm (Fig. 2B and  
93 2C). No endoplasmic reticulum envelopment was present around mitochondria, which is  
94 characteristic of some heterolobosean genera such as *Pharyngomonas*, *Stephanopogon*,  
95 *Percolomonas* or *Pleurostomum* (Supplementary Fig. 3; Pánek et al., 2017) No dictyosomes  
96 could be clearly distinguished. One can observe large digestive vacuoles that seem to  
97 correspond to different maturation stages (Fig 2A and 2D), from the phagosome containing  
98 bacteria to multilamellar bodies (MLB) (Hohl, 1965). MLB have been already described for  
99 the social amoeba *Dictyostelium discoideum* (Paquet et al., 2013) as well as for the ciliate  
100 *Tetrahymena pyriformis* (Trigui et al., 2016), both of which secrete them when fed on bacteria.  
101 This isolate produced round-shaped multilayered cysts (Fig. 2E and 2G). The thickness of the  
102 different layers did not appear regular and small vesicles were clearly apparent between the  
103 endo- and ectocyst (Fig. 2F and 2H). Vesicles surrounding the cysts (crypts), observed in  
104 optical microscopy, seem to be in fact expelled MLB that remain attached to the cyst wall.

105 *Euplaesiobystra dzianiensis* DD2

### 106 **Morphology and Ultrastructure**

107 *Euplaesiobystra dzianiensis* trophozoites ( $22 \pm 4.2 \mu\text{m}$  long (between 16.7 and 34  $\mu\text{m}$ ),  $13 \pm$   
108  $3.4 \mu\text{m}$  wide (between 8 and 20.6  $\mu\text{m}$ ) displayed a canonical heterolobosean morphology, being  
109 limax-shaped, monopodial and forming eruptive pseudopodia (Fig. 3A). Sometimes, a bulbous  
110 uroid with fine filaments (Fig. 3B and 3C) can be observed when trophozoites are in motion.

111 This FLA formed pleomorphic cysts which were mostly spherical ( $9.5 \pm 0.9 \mu\text{m}$  diameter), but  
112 some showed irregular outlines (Fig. 3D-F). A distinct outer layer, corresponding to the  
113 ectocyst, was visible (Fig. 3E). Encystment of this strain wasn't homogenous in our growth  
114 conditions: even after several days of starvation, trophozoites were still present. Cysts shown  
115 on figure 3 originate from a one-month old culture and are surrounded by cellular debris,  
116 suggesting that a portion of the initial trophozoite population lysed. In addition, despite the  
117 documented ability of *Euplaesiobystra hypersalinica* (Park et al., 2009) to switch to a transient  
118 flagellated stage, we were unable to observe such stage in our growth conditions.

119 *Euplaesiobystra dzianiensis* DD2 (Fig. 4) trophozoites contained one nucleus which displays  
120 a central nucleolus (Fig 4A). Electron-dense round shaped mitochondria (Fig. 4B) can be  
121 observed as well as numerous vacuoles, some of which contain bacteria probably undergoing  
122 digestion. No dictyosomes could be clearly distinguished, but some vacuoles displayed  
123 structural features resembling those of MLB, which are also present within the extracellular  
124 environment (Fig. 4C). Cysts harbored an irregular shape and thin but distinct ectocyst  
125 compared to a thick fibrillar endocyst (Fig. 4D). Within cysts, lipid droplets can be  
126 distinguished as well as some vesicles. A plugged ostiole was clearly observable (Fig. 4G), and  
127 some cysts displayed two pores (Fig. 4E). These observations are in line with previous work  
128 which documented the possible presence of 2 or more pores per cyst for *Euplaesiobystra*  
129 *hypersalinica* (Park et al., 2009). Within crescent-shaped cysts, cytoplasm in the vicinity of the  
130 cyst wall was highly vesiculated, hinting at export towards the cyst wall, while the plasma  
131 membrane was clearly distinguishable in the "rounded" cyst (Fig. 5D). These elements  
132 suggested that crescent cysts could be still encysting compared to rounded ones which would  
133 be more mature.

#### 134 **Molecular phylogeny of *Pharyngomonas* sp. DD1 and *Euplaesiobystra dzianiensis* DD2**

135 Two morphotypes of amoebae were isolated from the lake water after plate cultivation and  
136 liquid subcultures. To identify these isolates, DNA was extracted and 18S rRNA gene was  
137 sequenced. The 18S rRNA gene sequence of the first isolate DD1 (3136 bp) was compared to  
138 the nr database with BLAST, showing that the best hits (E-value = 0.0) corresponded to two  
139 *Pharyngomonas* sequences (i.e. *Pharyngomonas turkanaensis* LO and *Pharyngomonas* sp. RL)  
140 with 96% and 94% identity, respectively. A 983 bp group I intron was identified in the 18S  
141 rRNA sequence at position 583. Phylogeny confirmed this isolate belongs to the  
142 *Pharyngomonas* genus and is consequently referred to as *Pharyngomonas* sp. DD1 (Fig. 5).  
143 The helix 17-1 of 18S V3 region, a characteristic feature of Tetramitia was not present in

144 *Pharyngomonas* sp. DD1 rRNA gene sequence, consistent with its phylogenetic placement  
145 within *Pharyngomonas* (Supplementary Fig. 1 ; Nikolaev et al., 2004).

146 The 18S rRNA gene sequence of the second isolate DD2 (1846 bp) was confronted to the nr/nt  
147 database with BLAST, showing that the best hits (E-value = 0) corresponded to a partial 18S  
148 sequence from an uncultured heterolobosean isolate CBN AP20 (92% identity) and  
149 *Euplaesiobystra hypersalinica* strain A2 (85% identity). In addition to this moderate sequence  
150 homology, the determined phylogenetic positioning of this isolate suggests that it represents a  
151 new, distinct species related to *Euplaesiobystra hypersalinica*, the closest matching organism  
152 identified using 18S rRNA gene sequence (Fig. 5). It is therefore likely to represent a new  
153 species that we propose to name *Euplaesiobystra dzianiensis* sp. nov. (see taxonomic summary).  
154 Because the CBN AP20 sequence is significantly shorter than the other *Euplaesiobystra* ones,  
155 we excluded it from the main phylogenetic analysis. Inclusion of this sequences confirmed that  
156 isolate CBN AP20 is the closest relative to *E. dzianiensis* (Supplementary Fig. 2). As expected  
157 from its phylogenetic position, the *E. dzianiensis* DD2 rRNA gene sequence does include the  
158 ‘helix 17-1’ element characteristic of Tetramitia (Supplementary Fig. 1).

## 159 *Ecology*

### 160 **Amoeba isolates distribution in the lake**

161 In previous studies, it has been reported that the season and/or the depth in the lake can  
162 influence its microbial diversity (Bernard et al., 2019; Hugoni et al., 2018). To see whether the  
163 two FLA isolates were influenced by these parameters, we performed a specific qPCR on DNA  
164 isolated from the water lake sampled in April (end of the rainy season) and November (dry  
165 season) 2015. *Pharyngomonas* sp. DD1 concentration increased in November as compared to  
166 April (Fig. 6). This FLA concentration decreased with the depth, with the same pattern as  
167 photosynthetic microorganisms (e.g. cyanobacteria) below 5 m depth (Hugoni et al., 2018). *E.*  
168 *dzianiensis* DD2 showed an even more marked behaviour regarding seasonality since this  
169 isolate was almost not detected in April while it was present in all samples in November (Fig.  
170 6). It is also clear that its concentration decreased with the lake depth. These two isolates follow  
171 a similar trend of seasonal and depth distributions, being found in higher concentrations during  
172 dry season in shallow waters of lake Dziani Dzaha.

### 173 **Salt and temperature tolerance**

174 The two FLA strains presently described were isolated from a thalassohaline lake showing  
175 constant high salinity (40-60 ‰) and temperatures up to 35°C (Leboulanger et al., 2017). Thus,

176 we performed in vitro experiments to evaluate their salt and temperature tolerance for growth  
177 as compared to the in situ environmental conditions. *Pharyngomonas* sp. DD1 growth was not  
178 affected by temperature between 25 and 37°C, while it was clearly inhibited at 43°C (Table 1).  
179 With respect to salinity, *Pharyngomonas* sp. DD1 grew faster within the range from 15 to 75  
180 ‰. Growth was diminished at 100 ‰ and totally inhibited at 150 ‰ in our conditions.

181 *Euplaesiobystra dzianiensis* DD2 growth was inhibited at 43°C (Table 1). Regarding salinity,  
182 *E. dzianiensis* DD2 grew faster within the 15 to 40 ‰ range. The growth was hampered at 75  
183 ‰ and fully inhibited at 100 ‰ in our conditions. Ultimately, the two isolates displayed a  
184 similar behaviour regarding temperature, with a growth optimum ranging between 25 and  
185 37°C, while *E. dzianiensis* was less halotolerant than *Pharyngomonas*.

### 186 ***Euplaesiobystra dzianiensis* DD2 and *Pharyngomonas* sp. DD1 are able to phagocytose**

#### 187 **Arthrospira**

188 The spirulina *Arthrospira fusiformis* is the most abundant cyanobacterium in the lake,  
189 accounting for 95 % of the total photosynthetic biomass (Bernard et al., 2019). Its presence has  
190 been positively correlated with the temperature (Bernard et al., 2019). As the highest  
191 temperatures, as well as highest light intensity, were found in the upper layer of the water  
192 column (first three meters), *A. fusiformis* is mainly found within this level. Because amoebae  
193 were shown in this study to follow the same distribution pattern, grazing capacity of the two  
194 isolates on cyanobacterial prey was addressed. Grazing experiments, using culture of *A.*  
195 *fusiformis* isolated from the lake, were performed by mixing cyanobacteria and FLA in a single  
196 culture. *Euplaesiobystra dzianiensis* grazing on *Arthrospira* was observed (Fig. 7). It appeared  
197 that *E. dzianiensis* was able to ingest an *Arthrospira* filament, of almost the same size as itself  
198 (Fig. 7A). *A. fusiformis* parts could be observed in the majority of screened trophozoites. The  
199 same experiment was performed with *Pharyngomonas* sp. DD1 and *Arthrospira* pieces were  
200 also clearly observed in several trophozoite cells (Fig. 8).

## 201 **Discussion**

202 The thalassohaline lake of Dziani dzaha is considered an extreme environment of interest as it  
203 mimics environmental conditions that could be found in Precambrian oceans (Bernard et al.,  
204 2019). It could thus provide a window into early adaptation of microorganisms to such  
205 environmental conditions. Free-living amoebae belonging to the Heterolobosea have been  
206 repeatedly isolated in a variety of extreme environments with physicochemical properties that

207 are somewhat similar to what is found in the lake Dziani dzaha (Pánek et al., 2017). This  
208 prompted us to look for amoebae in this thalassohaline lake.

209 The two amoebae presently described were not detected by the previous metabarcoding study  
210 of the lake (Hugoni et al., 2018). This result might be partly due to a low and fluctuating  
211 abundance of these amoebae within the eukaryotic community of the lake or by the use of the  
212 universal 18S primers (515F and 951R) (Hugoni et al., 2018), which might not match the 18S  
213 rRNA gene sequence of the amoebae isolates. To check this hypothesis, the primers were tested  
214 with the SILVA database allowing three mismatches, without any in the last three nucleotides,  
215 to inspect the sequence coverage among eukaryotes. The primer pair matched 92% of the  
216 eukaryotic sequences within the SILVA database, showing their universality, however they did  
217 not match any heterolobosean sequences. Our analysis confirmed that heteroloboseids are  
218 highly likely to be missed using the 515F-951R 18S rRNA gene primers.

219 One amoeba isolated belongs to the *Pharyngomonas* genus and displayed morphological as  
220 well as genetic features that are hallmarks of this genus. Appending the size data collected by  
221 Park and Simpson (Park and Simpson, 2016 ; Supplementary Table 1), it appears that our strain  
222 is closer to *Pharyngomonas turkanaensis* in terms of size and shape of trophozoites and cyst  
223 than from *P. kirbyi* and other isolates. Such observations were supported by the phylogeny  
224 reconstructed from 18S rRNA gene sequences, showing that *P. turkanaensis* is the closest  
225 relative to *Pharyngomonas* sp. DD1. The comparison of morphological features highlighted  
226 that endocysts and ectocysts seemed thicker for *Pharyngomonas* sp. DD1 than for other  
227 described genus members. This might be due to vesicles/crypts, surrounding the cysts,  
228 observed in optical microscopy. Such vesicles seem in fact to be expelled multilamellar bodies  
229 (MLB) which stay attached to the cyst. They look different from previous observations which  
230 reported the presence of bacteria and/or fungi within these crypts (Park and Simpson, 2016).  
231 These authors also mentioned “scrolling feature within ectocyst (presumed fixation artifact)”  
232 which resemble what we consider as MLB surrounding *Pharyngomas* sp. DD1 cysts, but  
233 probably not an artefact. The moderate sequence divergence and the morphological difference  
234 of cyst structure between *P. turkanaensis* and *Pharyngomonas* sp. DD1 are not sufficient, in  
235 our opinion, to formally propose a new species.

236 The other isolated amoeba represents a new species of the *Euplaesiobystra* genus. The  
237 morphology and ultrastructure of this isolate is consistent with previous account of  
238 *Euplaesiobystra hypersalinica* (Park et al., 2009). Sequence comparison and phylogenetic

239 analyses highlighted a marked genetic divergence, with only a moderate identity to  
240 *Euplaesiobystra hypersalinica* strain A2 (85% identity). While morphology and phylogeny  
241 confidently group this isolate with *Euplaesiobystra*, it also clearly highlights a marked  
242 divergence from all other isolates, thus motivating the proposal of the novel species *E.*  
243 *dzianiensis*. Sequence comparison to the nr/nt database of the NCBI also revealed a high  
244 identity (92%) to a short, partial sequence of an heterolobosean isolate designated as CBN  
245 AP20. Phylogenetic inferences based on these short fragments confirmed that isolate CBN  
246 AP20 is the closest relative of *E. dzianiensis*. The CBN AP20 isolates was recently reported as  
247 a contaminant in spirulina production cultures (Yuan et al., 2018).

248 Our inability to identify a flagellate stage for both isolates and especially for *Pharyngomonas*,  
249 for which such a stage has been well described may be attributed to the way the strains were  
250 isolated (Park and Simpson, 2011; Plotnikov et al., 2015). Other authors used clonal liquid  
251 dilutions from environmental samples; in this study, we used agar plate isolation method, thus  
252 starting from trophozoites. After that, strains were propagated in flasks in ASW supplemented  
253 with a high density of *E. coli*: it may be possible that these conditions, while allowing quick  
254 and efficient growth of the amoeba stage, are not well suited to promote flagellation as has  
255 been reported for other Heterolobosea such as *Naegleria* (De Jonckheere, 2011). Some  
256 heterolobosea like *Marinamoeba* (De Jonckheere et al., 2009), only possess an amoebae stage,  
257 while others, like *Percolomonas* and *Stephanopogon* (Cavalier-Smith and Nikolaev, 2008) are  
258 only described as flagellates. Taking this into account, the recent characterization of  
259 *Pharyngomonas turkanaensis* suggested this isolate might be unable to adopt a flagellate stage  
260 (Park and Simpson, 2016). Ultimately, it might be that the ability to adopt a flagellate stage is  
261 not a conserved trait within the *Pharyngomonas* genus.

262 Because *Pharyngomonas* and *Euplaesiobystra* spp. were previously described as being able to  
263 grow in high salinity conditions, we tested this ability on both new isolates. *Pharyngomonas*  
264 sp. DD1 is able to grow between 15 and 100 ‰, which is consistent with its natural  
265 environment whose salinity varies between 34 and 71 ‰ (Hugoni et al., 2018). Interestingly,  
266 this result on salinity is quite similar to those observed with *P. turkanaensis* LO with a highest  
267 growth rate between 15 and 30 ‰ salinity and a cessation of growth by 125 ‰, although the  
268 latter strain has been isolated from the Turkana lake presenting a low salinity of about 4 ‰  
269 (Park and Simpson, 2016). These values are substantially lower than the ones observed for  
270 *Pharyngomonas kirbyi* SD1A and AS12B (75-250 ‰) (Park and Simpson, 2011), and  
271 *Pharyngomonas* sp. RL (50-250 ‰) (Harding et al., 2013). *Pharyngomonas* sp. DD1 thus

272 seems also far less halophilic than these strains. *Pharyngomonas* sp. DD1 is another example  
273 of a halotolerant isolate in the clade of Pharyngomonada, as *Tulamoeba bucina* (Kirby et al.,  
274 2015) is within the Tulamoebidae.

275 Compared to its closest relative in the literature, *i.e.* *Euplaesiobystra hypersalinica*, whose  
276 optimal growth salinity is around 150-200 ‰ (Park et al., 2009), *E. dzianiensis* DD2 was  
277 clearly less halotolerant. The two *Euplaesiobystra hypersalinica* isolates which have been  
278 described in the literature, originated from a hypersaline solar saltern (Park et al., 2009) (growth  
279 between 100 and 300 ‰) or from a lagoon (Park and Simpson, 2015) (290 ‰ in the originating  
280 sample). The third, which was first named *Plaesiobystra hypersalinica*, also originates from a  
281 hypersaline (140 ‰) environment (Park et al., 2009). The salinity tolerances of *Euplaesiobystra*  
282 *dzianiensis* and its closest relative, the heterolobosean CBN AP20, which has been isolated  
283 from cultures in Zarrouk medium (Zarrouk, 1966) whose salinity is about 20 ‰, suggests that  
284 these isolates are adapted to mesohaline rather than hypersaline environments.

285 qPCR assays were designed in order to investigate the presence and relative abundance of both  
286 amoebae in the lake Dziani Dzaha. Overall, they were found in higher relative abundance  
287 during the dry season (November), as compared to the rainy season (April). This pattern was  
288 particularly marked for *E. dzianiensis*, which was mostly undetected by qPCR in the rainy  
289 season. Additionally, the relative abundance of both amoebae decreased along an increasing  
290 water depth gradient. Thus, both amoebae seemed to be more abundantly found in surface  
291 water, regardless of the season. Such distribution patterns coincide with those of photosynthetic  
292 microorganisms of the lake Dziani Dzaha, such as the cyanobacterium *Arthrospira fusiformis*.  
293 Amoebae usually feed on smaller microorganisms that are ingested through phagocytosis.  
294 However, a few examples of amoebae feeding on larger preys are documented, such as  
295 *Vampyrella* spp. and *Leptophrys vorax*, (Rhizaria, Endomyxa) which feed on algal preys larger  
296 than themselves (Hess et al., 2012). Based on this, we investigated the ability of *E. dzianiensis*  
297 DD2 and *Pharyngomonas* sp. DD1 to feed on *A. fusiformis*, which are characterized as being  
298 straight or slightly wavy cylindrical trichomes whose size ranged from 170 to 2390 µm  
299 (Cellamare et al., 2018) and represent the most abundant cyanobacteria in the lake Dziani  
300 dzaha. Microscopic observations confirmed that both amoebae were able to feed on *A.*  
301 *fusiformis*, despite the fact that those bacteria are elongated and cannot be internalized as a  
302 whole by the amoebae. One of the closest matching sequences in the nr database for *E.*  
303 *dzianiensis* is that of the uncultured heterolobosean isolate CBN AP20, which has recently been  
304 reported as a contaminant in spirulina production cultures (Yuan et al., 2018). Further, it was

305 shown that isolate CBN AP20 was able to graze on the spirulina *Arthrospira*. Thus, such  
306 observation suggest that these amoebae may feed on cyanobacteria in natural conditions, using  
307 a mechanism that remains to be elucidated.

308 In conclusion, our study described a new FLA species among the Heterolobosea,  
309 *Euplaesiobystra dzianiensis* (DD2), and a new isolate of *Pharyngomonas* sp. (DD1), from the  
310 hypersaline lake Dziani Dzaha. Their growth in vitro was optimal at 25-37°C and around 40  
311 psu salinity, with a better tolerance to higher salinity for *Pharyngomonas*. Their abundances  
312 varied depending on the season and on the depth. Finally, we show that both isolates were able  
313 to phagocytose *A. fusiformis*, which is the predominant photosynthetic microorganism found  
314 in the lake. It would be interesting to examine whether other amoebae could be found in the  
315 lake and to better characterize the trophic interactions between these organisms and their preys.

## 316 **Taxonomic summary**

317 Assignment: Eukaryota; Excavata; Discoba; Discicristata; Heterolobosea; Tetramitida;  
318 *Euplaesiobystra*

319 *Euplaesiobystra dzianiensis* n. sp

320 Diagnosis: Heterolobosean, limax-shaped amoeba, capable of forming cysts. Single nucleus.  
321 Found in hypersaline habitat. Trophozoites: 17-33 µm (average: 22 µm) and 8-20 µm (average:  
322 13 µm) in length and width; sometimes with uroid and uroidal filaments during motion.  
323 Frequent eruptive movements. Cyst: spherical or crescent shaped; 9.5 µm in diameter, 1-2  
324 observed plugged pores, wall with distinct ectocyst and endocyst. Growth in salinities ranging  
325 from 15 to 75 ‰. Flagellate phase unknown.

326 Type material: two samples have been deposited as the name-bearing type (an hapantotype) in  
327 the protist collection of the National Museum of Natural History, Paris. The first is a culture of  
328 isolate DD2, preserved in ethanol 70 % (accession number MNHN-IR-2020-03), the second is  
329 a cyst suspension (accession number MNHN-IR-2020-04).

330 Type locality: type culture isolated from the thalassohaline lake Dziani Dzaha located in the  
331 Petite Terre island in Mayotte (12°46'15.6" S; 45°17'19.2" E).

332 Etymology: The species epithet “*dzianiensis*” refers to the lake Dziani Dzaha from which the  
333 sample is originating (-ensis).



334 Gene sequence. The 18S rRNA gene sequence from *Euplaesiobystra dzianiensis* isolate DD2  
335 has the Genbank Accession number MN969059.

336 Zoobank registration Described under the Zoological Code; Zoobank registration  
337 urn:lsid:zoobank.org:act:53D12014-6E7B-4D87-8080-691FB443CB1F

338 This work has been registered with Zoobank as urn:lsid:zoobank.org:pub:FAEA9268-8E01-  
339 4E33-AF36-039AF9436616

## 340 **Materials and methods**

### 341 *Isolation and cultivation of amoebae*

342 Water samples were taken from the lake Dziani Dzaha, located in the Petite Terre island in  
343 Mayotte (12°46'15.6" S; 45°17'19.2" E). The lake was sampled in April and November 2015,  
344 along a depth profile (0.25 m, 1 m, 2.5 m, 5 m, 11 m, 15 m and 17 m depth) located above the  
345 deepest point of the lake, using a horizontal 1.2-L Niskin bottle (Hugoni *et al.* 2018). The lake  
346 Dziani Dzaha presents peculiar features such as high salinity (around 52 psu), high pH (9 to  
347 9.5) and high temperature (27 to 35°C).

348 A water sample (100 ml) was filtered on a sterile Nucleopore polycarbonate filter (3 µm pore  
349 size; 47 mm diameter) using a vacuum pump. The filter was cut in two pieces and deposited  
350 onto saline non-nutrient agar (NaCl 60 g/L, Sodium Citrate tribasic 0.8 g/L, MgSO<sub>4</sub> 4 mM,  
351 Na<sub>2</sub>HPO<sub>4</sub> 2.5 mM, KH<sub>2</sub>PO<sub>4</sub> 2.5 mM, CaCl<sub>2</sub> 0.5 mM) seeded with 100 µL of an *Escherichia*  
352 *coli* suspension (*E. coli* were grown overnight in Lysogeny Broth - peptone 10 g/L, yeast  
353 extract 5 g/L, NaCl 10 g/L - , centrifuged for five minutes at 6000 g and resuspended in ASW  
354 to reach an optical density of about 50 when measured at 600 nm) (NNA-Eco plate). The plates  
355 were sealed with parafilm and incubated at 30°C until a migration front was observed. Fronts  
356 were excised from plates and used for re-isolation on an NNA-Eco plate or to inoculate flasks  
357 containing Artificial Sea Water (ASW: 26.29 g NaCl, 0.74 g KCl, 0.99 g CaCl<sub>2</sub>, 6.09 g  
358 MgCl<sub>2</sub>•6H<sub>2</sub>O, 3.94 g MgSO<sub>4</sub>•7H<sub>2</sub>O L<sup>-1</sup>, pH 7.8) seeded with a population of *E. coli* (the  
359 previously described suspension was diluted to one hundredth in the amoebae growth medium  
360 so that the optical density measured at 600 nm was approximately 0.5). Isolated amoebae were  
361 routinely grown in ASW-*E. coli* at 30°C.

### 362 *Cultivation of Arthrospira fusiformis*

363 *Arthrospira fusiformis* suspensions were a kind gift from Charlotte Duval. They have been  
364 grown at 25°C with a light intensity of 15 µmol photons m<sup>-2</sup> s<sup>-1</sup> with a 16 hours light/8 hours

365 dark cycles in Z8 Mayotte medium (per 1 L: 20 g NaCl, 0.467 g NaNO<sub>3</sub>, 59 mg  
366 Ca(NO<sub>3</sub>)<sub>2</sub>•4H<sub>2</sub>O, 25 mg MgSO<sub>4</sub>•7H<sub>2</sub>O, 31 mg K<sub>2</sub>HPO<sub>4</sub>, 21 mg Na<sub>2</sub>CO<sub>3</sub>, 10 mL Fe-EDTA  
367 solution (A: dissolve 2.8 g FeCl<sub>3</sub>•6H<sub>2</sub>O in 100 mL 0.1 N HCl, B: dissolve 3.9 g EDTA-Na<sub>2</sub> in  
368 0.1 M NaOH, add 10 ml solution A and 9.5 ml solution B plus water to 1 L), 1 mL trace solution  
369 (for 1L: 0.31 g H<sub>3</sub>BO<sub>3</sub>, 0.223 g MnSO<sub>4</sub>•4H<sub>2</sub>O, 0.89 mg V<sub>2</sub>O<sub>5</sub>, 3.3 mg Na<sub>2</sub>WO<sub>4</sub>•2H<sub>2</sub>O, 8.8 mg  
370 (NH<sub>4</sub>)<sub>6</sub>Mo<sub>7</sub>O<sub>24</sub>•4H<sub>2</sub>O, 12.1 mg KBr, 8.3 mg KI, 28.7 mg ZnSO<sub>4</sub>•7H<sub>2</sub>O, 15.5 mg  
371 Cd(NO<sub>3</sub>)<sub>2</sub>•4H<sub>2</sub>O, 14.6 mg Co(NO<sub>3</sub>)<sub>2</sub>•6H<sub>2</sub>O, 12.5 mg CuSO<sub>4</sub>•5H<sub>2</sub>O, 19.8 mg  
372 (NH<sub>4</sub>)<sub>2</sub>Ni(SO<sub>4</sub>)<sub>2</sub>•6H<sub>2</sub>O, 4.1 mg Cr(NO<sub>3</sub>)<sub>3</sub>•9H<sub>2</sub>O, 47.4 mg Al<sub>2</sub>(SO<sub>4</sub>)<sub>3</sub>K<sub>2</sub>SO<sub>4</sub>•24H<sub>2</sub>O), Cultures  
373 were not axenic but have been passed in aseptic conditions.

#### 374 *Microscopy*

375 Cultures of FLA at different developmental stages were transferred into 35 mm dishes with  
376 glass coverslips (μ-dish, Ibidi). The cells were left to adhere at room temperature and observed  
377 using an inverted microscope equipped with differential interference contrast (DIC)  
378 (Olympus). Images' contrast and brightness were further adjusted using ImageJ. DIC  
379 micrographs were used to evaluate cell sizes, which are expressed at mean values ± standard  
380 deviation (40 trophozoites and 20 cysts were measured for each strain). For cyanobacterial  
381 grazing assays, images were acquired using an inverted brightfield microscope. For  
382 transmission electron microscopy, FLA cultures in their trophozoite or cyst stages were fixed  
383 by incubating the culture in ASW or 60‰ artificial salinity medium (see “Salinity and  
384 temperature tolerance” for composition) containing a final concentration of 2.5%  
385 glutaraldehyde for 1 hour at 4°C. Cells were rinsed three times in phosphate buffer (0.1 M, pH  
386 7.2) and post-fixed in a 1% osmium tetroxide solution, for 1 hour at 4°C. Cells were rinsed,  
387 embedded in Histogel for further handling. Cells were dehydrated in increasing acetone bath  
388 (50%, 70%, 90%, 100%) and embedded, first in a mix of acetone and araldite resin (1:1) for  
389 one hour, then in pure araldite and left to harden for approximately 24 h. Ultrathin section (70  
390 nm) were stained with 4% uranyl acetate and lead citrate, and observed using JEOL 1010  
391 transmission electron microscope operating at 75 kV.

#### 392 *Molecular identification*

393 Nucleic acids were extracted from cultivated isolates using Microbial Genomic DNA kit  
394 (Macherey-Nagel), according to manufacturer's recommendations. Primers ACA-5'  
395 (CTGGTTGATCCTGCCAGTAGTC) and ACA-3' (TGATCCTTCCGCAGGTTTAC) were  
396 used to amplify 18S rRNA gene with Phusion DNA polymerase (ThermoFisher) with the  
397 following parameters: 98°C for 30 sec, followed by 35 cycles comprising: 98°C for 10 sec,

398 65°C for 30 sec, 72°C for 1 min, then a final elongation step of 5 min at 72°C. The amplicons  
399 were sequenced by the Sanger method. The sequences have been deposited within GenBank  
400 under the accession numbers MN969060 and MN969059 for isolates DD1 and DD2  
401 respectively.

#### 402 *Phylogenetic analysis*

403 A collection of full length or near full-length sequences belonging to Heterolobosea were  
404 retrieved from the NCBI nucleotide database, along with Euglenozoa sequences for  
405 constituting an outgroup. Sequences were aligned using MUSCLE (Edgar 2004). Alignment  
406 was manually inspected, in order to eliminate regions corresponding to intronic sequences and  
407 to trim sequences to begin and end on same positions. Sequences alignment was further cleaned  
408 using BMGE, resulting in an alignment spanning 1671 nucleotides, comprising 46 sequences  
409 (Criscuolo and Gribaldo 2010). Phylogeny inference was performed using IQ-Tree (Nguyen et  
410 al. 2015). The best substitution model was defined using ModelFinder, based on the highest  
411 Bayesian information criterion, which was found to correspond to the TIM2+R5 model. During  
412 tree inference, branch support was assessed using bootstrapping (1000 iterations) and an SH-  
413 like approximate likelihood ratio test. The resulting tree was rendered and further annotated  
414 using iTOL (Letunic and Bork 2019).

#### 415 *Quantitative PCR*

416 Quantitative PCR (qPCR) analysis was performed to detect *Pharyngomonas* sp. DD1 and  
417 *Euplaesiobystra dzianiensis* DD2, using primer pairs PharF1 5'-  
418 CGTATTACTGGGCGAGAGGTG-3', PharR1 5'-CGTTCCTGATTGACGGGAGAG-3' and  
419 GargF1 5'-CAGCGATCAAAGCGTAAGGAAG-3', GargR1 5'-  
420 CGTGCAGCCCAAGACATATTAG-3', respectively (primers were designed from 18S rRNA  
421 genes using Clone manager). Sampling of water from the lake Dziani Dzaha was performed in  
422 April and November 2015 and at various depths (Hugoni *et al.* 2018). DNA extraction was  
423 performed as described previously (Hugoni *et al.* 2018). qPCR was performed using the  
424 LightCycler 480 apparatus and FastStart DNA Master plus SYBR Green I according to  
425 manufacturer instructions (Roche Applied Science). The reactions were performed under the  
426 following conditions: an initial denaturation step of 95°C for 10 min, followed by 45 cycles:  
427 95°C for 10 s, 60°C for 10 s, and 72°C for 10 s. To verify the specificity of the amplicon for  
428 each primer pair, a melting curve analysis was performed ranging from 65°C to 95°C.

## 429 *Salinity and temperature tolerance*

430 Salinity and temperature tolerance of both strains were investigated by inoculating 50 µl of  
431 actively growing stock cultures in ASW (trophozoites were dividing, no cysts were observable)  
432 in 1 mL of various salinity media based on 300‰ artificial salinity medium (272 g NaCl, 7.6  
433 g KCl, 17.8 g MgCl<sub>2</sub>, 1.8 g MgSO<sub>4</sub>·7H<sub>2</sub>O, 1.3 g CaCl<sub>2</sub> l<sup>-1</sup> water (Park 2012)) in a 24-well  
434 plate. Dilutions in ASW, 15‰, 40‰, 75‰, 100‰ and 150‰ were seeded with *E. coli* (~5.10<sup>8</sup>  
435 cells). *E. coli* (~5.10<sup>8</sup> cells) were added every 48 or 72h for ten days to limit encystment.  
436 Growth was microscopically monitored every 24 or 48h at 25, 30, 37 or 43°C, by looking for  
437 actively moving amoebae and increase of the populations density. After ten days, growth was  
438 confirmed by transferring 50 µL of each culture into 1 ml of the same medium and subsequent  
439 observations for ten days (adding *E. coli* (~5.10<sup>8</sup> cells) every 48 or 72h. All tests were  
440 performed twice.

## 441 *Arthrospira grazing tests*

442 Suspensions of *Arthrospira fusiformis* were kindly provided by Cécile Bernard. Bacteria were  
443 diluted 1/10th in 1 mL of ASW (in 24-wells plate) and inoculated 1/100th with an actively  
444 growing culture of amoebae. Mixtures were grown at 30°C and observed under an Olympus  
445 IX51 microscope equipped with an Olympus DP26 camera.

## 446 **Acknowledgments**

447 The authors thanks Cécile Bernard and Charlotte Duval for providing the cyanobacteria culture  
448 for the grazing study. The field permit was granted by the Conservatoire du Littoral et des  
449 Rivages Lacustres, Antenne Océan Indien, due to the fact that the lake Dziani Dzaha is  
450 currently a protected water body with free public access but restricted activities, under the  
451 control of the French agency for littoral ecosystems conservation ([http://www.conservatoiredu-](http://www.conservatoiredu-littoral.fr/)  
452 [littoral.fr/](http://www.conservatoiredu-littoral.fr/)).

## 453 **Authors contribution**

454 Willy Aucher: Conceptualization, Methodology, Validation, Investigation, Visualization,  
455 Writing

456 Vincent Delafont: Conceptualization, Investigation, Data Curation, Formal  
457 analysis, Visualization, Writing

458 Elodie Ponlaitiac: Investigation

459 Aurélien Alafaci: Investigation  
460 Hélène Agogué: Resources  
461 Christophe Leboulanger: Resources  
462 Marc Bouvy: Resources, Writing  
463 Yann Héchard: Conceptualization, Supervision, Writing

## 464 **Funding**

465 This work was partly funded by the European Union and the region of Nouvelle Aquitaine  
466 through the “Habisan program” (CPER-FEDER). This work was partly funded by Agence  
467 Nationale de la Recherche (project DZIANI, grant number ANR-13-BS06-0001), Total  
468 Corporate Foundation (project DZAHA C001493). The funders had no role in study design,  
469 data collection and analysis, decision to publish, or preparation of the manuscript.

## 470 **References**

- 471 Baumgartner, M., Eberhardt, S., De Jonckheere, J.F., Stetter, K.O., 2009. *Tetramitus*  
472 *thermacidophilus* n. sp., an amoeboflagellate from acidic hot springs. *J. Eukaryot.*  
473 *Microbiol.* <https://doi.org/10.1111/j.1550-7408.2009.00390.x>
- 474 Bernard, C., Escalas, A., Villeriot, N., Agogué, H., Hugoni, M., Duval, C., Carré, C., Got, P.,  
475 Sarazin, G., 2019. Very Low Phytoplankton Diversity in a Tropical Saline-Alkaline  
476 Lake , with Co-dominance of *Arthrospira fusiformis* ( Cyanobacteria ) and *Picocystis*  
477 *salinarum* ( Chlorophyta ).
- 478 Cavalier-Smith, T., Nikolaev, S., 2008. The zooflagellates *Stephanopogon* and *Percolomonas*  
479 are a clade (class percolatea: Phylum percolozoa). *J. Eukaryot. Microbiol.*  
480 <https://doi.org/10.1111/j.1550-7408.2008.00356.x>
- 481 Cellamare, M., Duval, C., Drelin, Y., Djediat, C., Touibi, N., Agogué, H., Leboulanger, C.,  
482 Ader, M., Bernard, C., 2018. Characterization of phototrophic microorganisms and  
483 description of new cyanobacteria isolated from the saline-alkaline crater-lake Dziani  
484 Dzaha (Mayotte, Indian Ocean). *FEMS Microbiol. Ecol.* 94.  
485 <https://doi.org/10.1093/femsec/fiy108>
- 486 De Jonckheere, J.F., 2014. What do we know by now about the genus *Naegleria*? *Exp.*  
487 *Parasitol.* <https://doi.org/10.1016/j.exppara.2014.07.011>
- 488 De Jonckheere, J.F., 2011. Origin and evolution of the worldwide distributed pathogenic  
489 amoeboflagellate *Naegleria fowleri*. *Infect. Genet. Evol.*  
490 <https://doi.org/10.1016/j.meegid.2011.07.023>
- 491 De Jonckheere, J.F., Baumgartner, M., Opperdoes, F.R., Stetter, K.O., 2009. *Marinamoeba*  
492 *thermophila*, a new marine heterolobosean amoeba growing at 50 °C. *Eur. J. Protistol.*  
493 <https://doi.org/10.1016/j.ejop.2009.01.001>

- 494 Finlay, B.J., Curds, C.R., Bamforth, S.S., Bafort, J.M., 1987. Ciliated Protozoa and other  
495 Microorganisms from Two African Soda Lakes (Lake Nakuru and Lake Simbi, Kenya).  
496 Arch. fur Protistenkd. 133, 81–91. [https://doi.org/10.1016/S0003-9365\(87\)80041-6](https://doi.org/10.1016/S0003-9365(87)80041-6)
- 497 Harding, T., Brown, M.W., Plotnikov, A., Selivanova, E., Park, J.S., Gunderson, J.H.,  
498 Baumgartner, M., Silberman, J.D., Roger, A.J., Simpson, A.G.B.B., 2013. Amoeba  
499 Stages in the Deepest Branching Heteroloboseans, Including Pharyngomonas:  
500 Evolutionary and Systematic Implications. Protist 164, 272–286.  
501 <https://doi.org/10.1016/j.protis.2012.08.002>
- 502 Hess, S., Sausen, N., Melkonian, M., 2012. Shedding light on vampires: the phylogeny of  
503 vampyrellid amoebae revisited. PLoS One 7, e31165.  
504 <https://doi.org/10.1371/journal.pone.0031165>
- 505 Hohl, H.R., 1965. Nature and Development of Membrane Systems in Food Vacuoles of  
506 Cellular Slime Molds Predatory upon Bacteria. J. Bacteriol.  
507 <https://doi.org/10.1128/jb.90.3.755-765.1965>
- 508 Hugoni, M., Escalas, A., Bernard, C., Nicolas, S., Jézéquel, D., Vazzoler, F., Sarazin, G.,  
509 Leboulanger, C., Bouvy, M., Got, P., Ader, M., Troussellier, M., Agogué, H., 2018.  
510 Spatiotemporal variations in microbial diversity across the three domains of life in a  
511 tropical thalassohaline lake (Dziani Dzaha, Mayotte Island). Mol. Ecol. 4775–4786.  
512 <https://doi.org/10.1111/mec.14901>
- 513 Jhin, S.H., Park, J.S., 2019. A New Halophilic Heterolobosean Flagellate, *Aurem hypersalina*  
514 gen. n. et sp. n., Closely Related to the Pleurostomum - Tulamoeba Clade: Implications  
515 for Adaptive Radiation of Halophilic Eukaryotes. J. Eukaryot. Microbiol. 66, 221–231.  
516 <https://doi.org/10.1111/jeu.12664>
- 517 Kirby, W.A., Tikhonenkov, D. V., Mylnikov, A.P., Janouškovec, J., Lax, G., Simpson,  
518 A.G.B., 2015. Characterization of *Tulamoeba bucina* n. sp., an extremely halotolerant  
519 amoeboflagellate heterolobosean belonging to the Tulamoeba-Pleurostomum clade  
520 (*Tulamoebidae* n. fam.). J. Eukaryot. Microbiol. <https://doi.org/10.1111/jeu.12172>
- 521 Leboulanger, C., Agogué, H., Bernard, C., Bouvy, M., Carré, C., Cellamare, M., Duval, C.,  
522 Fouilland, E., Got, P., Intertaglia, L., Lavergne, C., Le Floc’h, E., Roques, C., Sarazin,  
523 G., 2017. Microbial Diversity and Cyanobacterial Production in Dziani Dzaha Crater  
524 Lake, a Unique Tropical Thalassohaline Environment. PLoS One 12, e0168879.  
525 <https://doi.org/10.1371/journal.pone.0168879>
- 526 Nikolaev, S.I., Mylnikov, A.P., Berney, C., Fahrni, J., Pawloski, J., Aleshin, V. V., Petrov,  
527 N.B., 2004. Molecular Phylogenetic Analysis Places *Percolomonas cosmopolites* within  
528 Heterolobosea: Evolutionary Implications. J. Eukaryot. Microbiol. 51, 575–581.  
529 <https://doi.org/10.1111/j.1550-7408.2004.tb00294.x>
- 530 Nougier, J., Cantagrel, J.M., Karche, J.P., 1986. The Comores archipelago in the western  
531 Indian Ocean: volcanology, geochronology and geodynamic setting. J. African Earth  
532 Sci. 5, 135–145. [https://doi.org/10.1016/0899-5362\(86\)90003-5](https://doi.org/10.1016/0899-5362(86)90003-5)
- 533 Pánek, T., Simpson, A.G.B., Brown, M.W., Dyer, B.D., 2017. Heterolobosea. Springer,  
534 Cham. <https://doi.org/10.1007/978-3-319-32669-6>
- 535 Paquet, V.E., Lessire, R., Domergue, F., Fouillen, L., Filion, G., Sedighi, A., Charette, S.J.,  
536 2013. Lipid composition of multilamellar bodies secreted by *Dictyostelium discoideum*  
537 reveals their amoebal origin. Eukaryot. Cell. <https://doi.org/10.1128/EC.00107-13>

- 538 Park, J.S., De Jonckheere, J.F., Simpson, A.G.B., 2012. Characterization of *Selenaion*  
539 *koniopes* n. gen., n. sp., an Amoeba that Represents a New Major Lineage within  
540 Heterolobosea, Isolated from the Wieliczka Salt Mine. *J. Eukaryot. Microbiol.* 59, 601–  
541 613. <https://doi.org/10.1111/j.1550-7408.2012.00641.x>
- 542 Park, J.S., Simpson, A.G.B., 2016. Characterization of a Deep-Branching Heterolobosean,  
543 *Pharyngomonas turkanaensis* n. Sp., Isolated from a Non-Hypersaline Habitat, and  
544 Ultrastructural Comparison of Cysts and Amoebae among *Pharyngomonas* Strains. *J.*  
545 *Eukaryot. Microbiol.* 63, 100–111. <https://doi.org/10.1111/jeu.12260>
- 546 Park, J.S., Simpson, A.G.B., 2015. Diversity of Heterotrophic Protists from Extremely  
547 Hypersaline Habitats. *Protist* 166, 422–437. <https://doi.org/10.1016/j.protis.2015.06.001>
- 548 Park, J.S., Simpson, A.G.B., 2011. Characterization of *Pharyngomonas kirbyi* (=   
549 “*Macropharyngomonas halophila*” nomen nudum), a Very Deep-branching, Obligately  
550 Halophilic Heterolobosean Flagellate. *Protist* 162, 691–709.  
551 <https://doi.org/10.1016/j.protis.2011.05.004>
- 552 Park, J.S., Simpson, A.G.B., Brown, S., Cho, B.C., 2009. Ultrastructure and Molecular  
553 Phylogeny of two Heterolobosean Amoebae, *Euplaesiobystra hypersalinica* gen. et sp.  
554 nov. and *Tulamoeba peronaphora* gen. et sp. nov., Isolated from an Extremely  
555 Hypersaline Habitat. *Protist* 160, 265–283. <https://doi.org/10.1016/j.protis.2008.10.002>
- 556 Park, J.S., Simpson, A.G.B., Lee, W.J., Cho, B.C., 2007. Ultrastructure and Phylogenetic  
557 Placement within Heterolobosea of the Previously Unclassified, Extremely Halophilic  
558 Heterotrophic Flagellate *Pleurostomum flabellatum* (Ruinen 1938). *Protist* 158, 397–  
559 413. <https://doi.org/10.1016/j.protis.2007.03.004>
- 560 Plotnikov, A.O., Mylnikov, A.P., Selivanova, E.A., 2015. Morphology and life cycle of  
561 amoeboflagellate *Pharyngomonas* sp. (Heterolobosea, Excavata) from hypersaline  
562 inland Razval Lake. *Biol. Bull.* 42, 759–769.  
563 <https://doi.org/10.1134/S1062359015090083>
- 564 Samba-Louaka, A., Delafont, V., Rodier, M.-H., Cateau, E., Héchard, Y., 2019. Free-living  
565 amoebae and squatters in the wild: ecological and molecular features. *FEMS Microbiol.*  
566 *Rev.* 1–20. <https://doi.org/10.1093/femsre/fuz011>
- 567 Trigui, H., Paquet, V.E., Charette, S.J., Faucher, S.P., 2016. Packaging of *Campylobacter*  
568 *jejuni* into multilamellar bodies by the ciliate *Tetrahymena pyriformis*. *Appl. Environ.*  
569 *Microbiol.* <https://doi.org/10.1128/AEM.03921-15>
- 570 Yuan, D., Zhan, X., Wang, M., Wang, X., Feng, W., Gong, Y., Hu, Q., 2018. Biodiversity  
571 and distribution of microzooplankton in *Spirulina* (*Arthrospira*) *platensis* mass cultures  
572 throughout China. *Algal Res.* 30, 38–49. <https://doi.org/10.1016/j.algal.2017.12.009>
- 573 Zarrouk, C., 1966. Contribution a l’etude d’une Cyanophyce. Influence de Divers Facteurs  
574 Physiques et Chimiques sur la croissance et la photosynthese de *Spirulina mixima*.  
575 Thesis. Univ. Paris, Fr.
- 576 Zinke, J., Reijmer, J.J., Thomassin, B., 2003. Systems tracts sedimentology in the lagoon of  
577 Mayotte associated with the Holocene transgression. *Sediment. Geol.* 160, 57–79.  
578 [https://doi.org/10.1016/S0037-0738\(02\)00336-6](https://doi.org/10.1016/S0037-0738(02)00336-6)

## 579 **Figure legends**

580 **Figure 1:** Differential interference contrast micrographs of *Pharyngomonas* sp. DD1 grown in  
581 Artificial Sea Water (ASW) liquid medium. The trophozoite stage can show a variety of shapes  
582 (A-D) while the cyst stage consistently shows round-shaped cells with a multilayered cell wall  
583 (E-F), surrounded by spherical, “bead-like” structures. Scale bar represents 10  $\mu\text{m}$  for all  
584 panels.

585 **Figure 2:** Transmission electron micrographs of *Pharyngomonas* sp. DD1. Trophozoite cells  
586 harbor numerous vacuoles, possibly arising from phagocytosis (A, B, C (detail from B), D).  
587 Cysts ultrastructure (E-H) confirms the presence of a spacious, thin multilayered wall, in which  
588 are embedded “bead-like” structures that appear to be host-derived multi-layered bodies  
589 (details F and H). Scale bar is 2  $\mu\text{m}$  for all panels.

590 **Figure 3:** Differential interference contrast micrographs of *Euplaesiobystra dzianiensis* DD2  
591 grown in ASW. *Euplaesiobystra dzianiensis* trophozoites are monopodial (A) and tend to  
592 branch when changing movement direction (B, C), showing rapid eruptive deployment of large  
593 pseudopodia. Cysts show an irregular, round-shaped morphology (D-F) with a double wall  
594 clearly observable (E). Scale bar represents 10  $\mu\text{m}$  for all panels

595 **Figure 4:** Transmission electron micrographs of *Euplaesiobystra dzianiensis* DD2.  
596 Trophozoites cells display a single nucleus with a large nucleolus, as well as numerous  
597 vacuoles seemingly indicating various stages of phagocytosis (A). Round shaped mitochondria  
598 with discoidal cristae (B; detail from A). Some intracellular vacuoles contain multi-layered  
599 bodies, which are then expelled in the extracellular medium (C). Cysts morphology of *E.*  
600 *dzianiensis* is variable, ranging from round to crescent shapes (D-F), always doubled-layered  
601 with a well-defined ectocyst. Prominent ostioles (D-G) can be easily seen on cyst cell walls.  
602 Scale bar is 2  $\mu\text{m}$  for all panels.

603 **Figure 5:** Phylogenetic tree of the Heterolobosea group, reconstructed using maximum  
604 likelihood (TIM2+R5 model). The FLA isolates newly described in the present study are  
605 indicated in bold. Branch supports, assessed using bootstrap (1000 iterations; left value) and  
606 an SH-like approximate likelihood ratio test (SH-ALRT; right value), are indicated at nodes  
607 with branches length  $> 0.05$ . Euglenozoa sequences were used as an outgroup. Scale bar shows  
608 the substitution rate per site. Environmental origin for sequences is indicated by coloured  
609 circles, when available.



610 **Figure 6:** Molecular quantification of FLA isolates in the lake Dziani Dzaha, using specific  
611 quantitative PCR assays. Absolute DNA concentrations in samples were determined at depths  
612 ranging from 0.25 m to 17 m, in either April (rainy season) or November (dry season) 2015.  
613 The black thick line represents the lower limit of quantification.

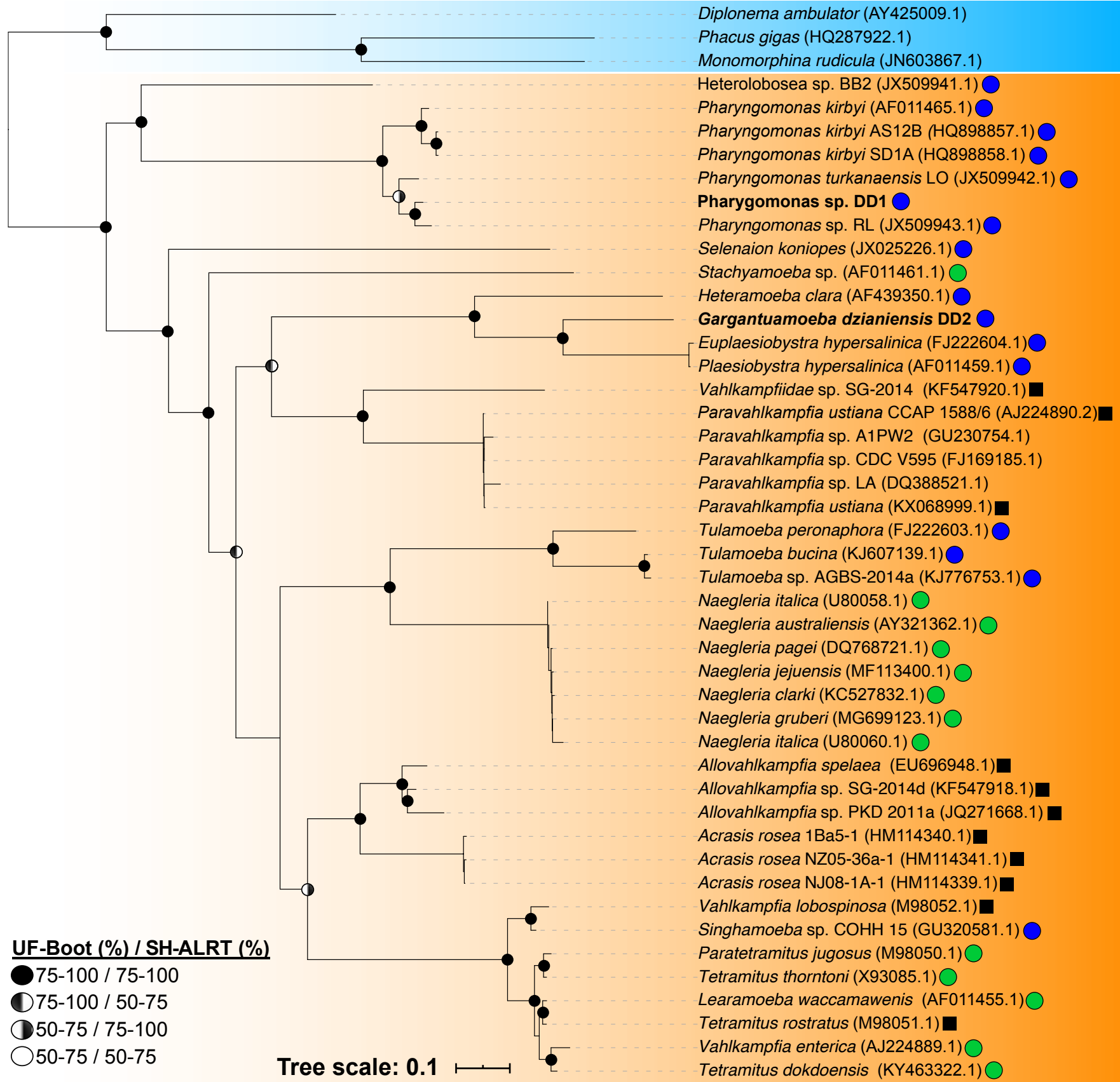
614 **Table 1:** Qualitatively estimated growth response to salinities and temperatures of  
615 *Pharyngomonas* sp. DD1 and *Euplaesiobystra dzianiensis* DD2. Table note: + = moderate  
616 growth, ++ = growth to high densities, - = no growth

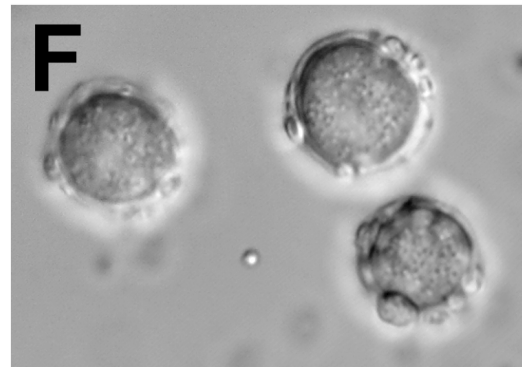
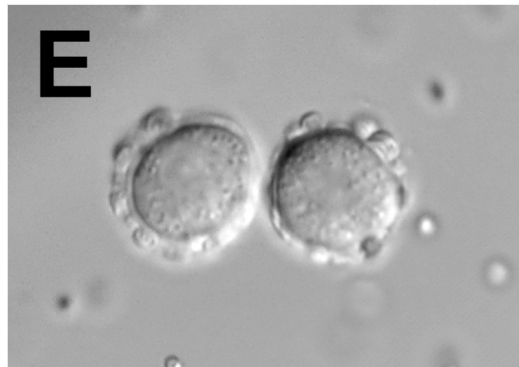
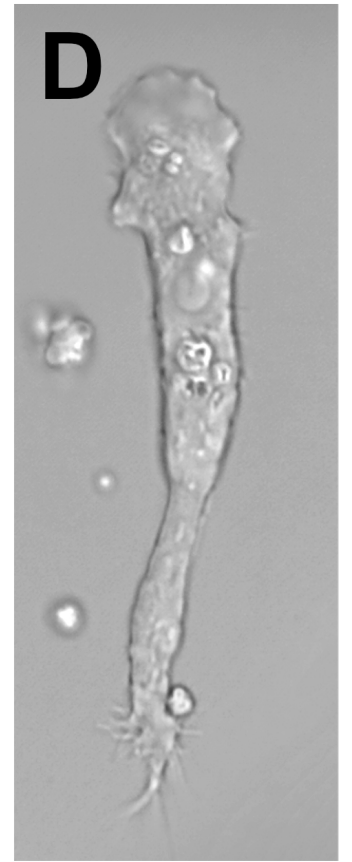
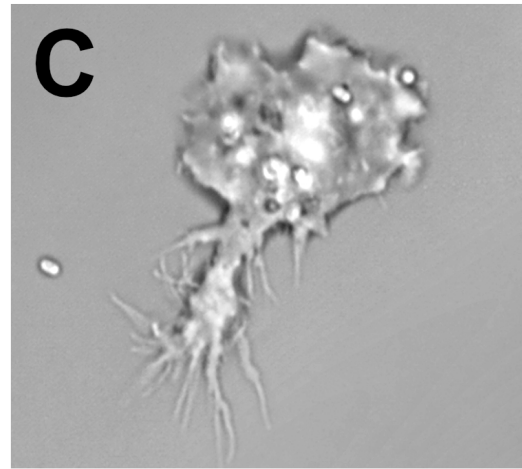
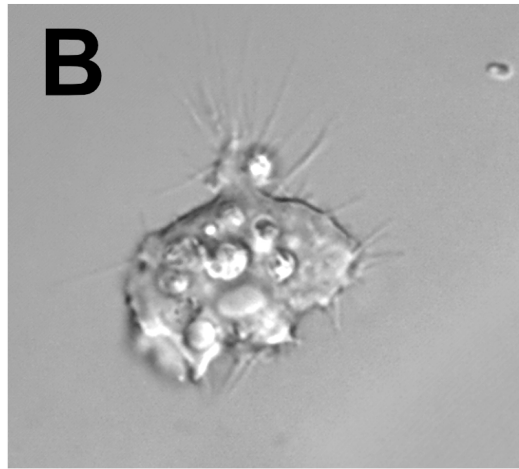
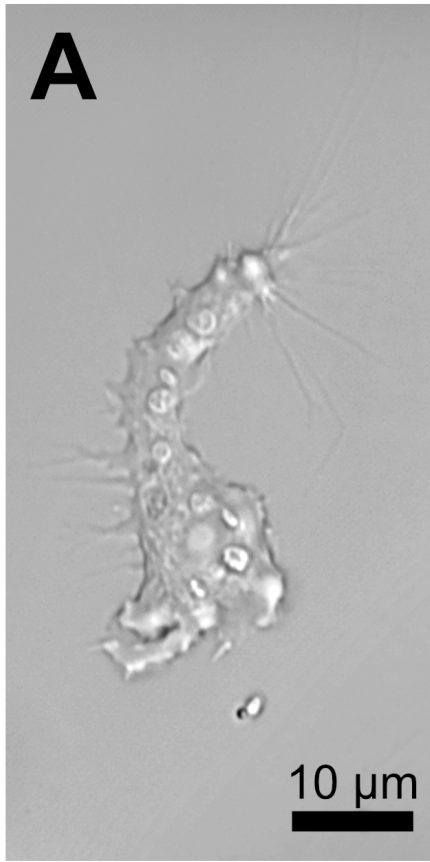
617 **Figure 7:** Light micrographs of *Euplaesiobystra dzianiensis* DD2 grazing on *Arthrospira*  
618 *fusiformis*. Whole cyanobacterial filaments (A) or vacuoles filled with cyanobacterial-derived  
619 contents (B) were observed in trophozoite cells of *E. dzianiensis*. Scale bar is 20  $\mu$ m for both  
620 panels.

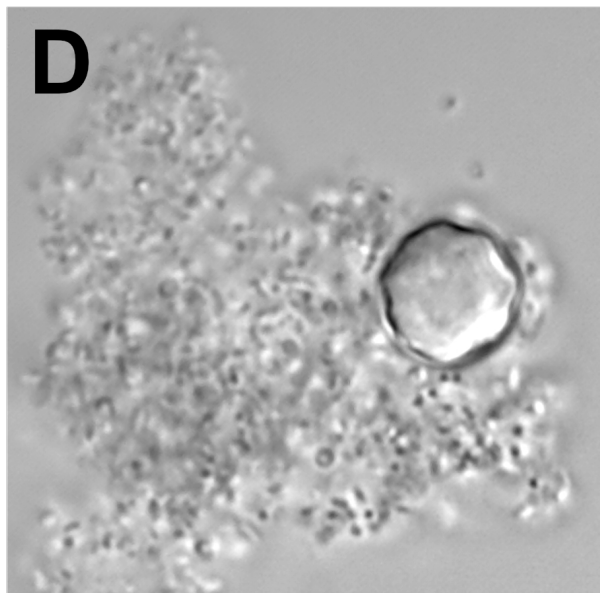
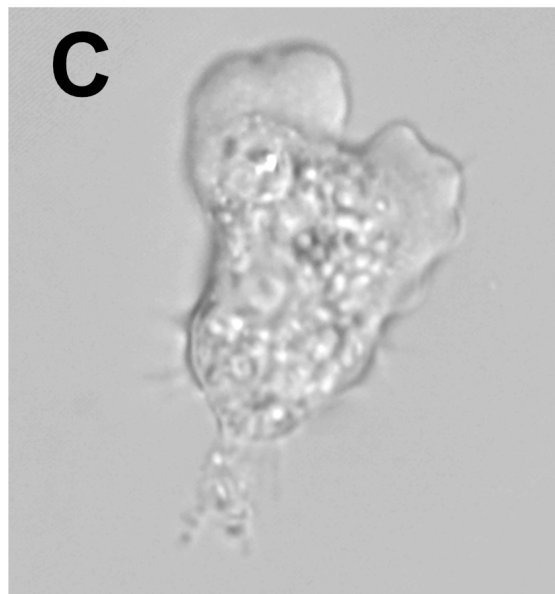
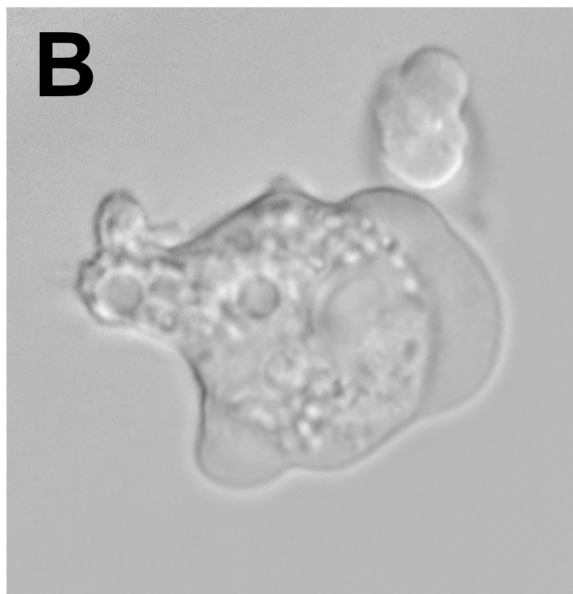
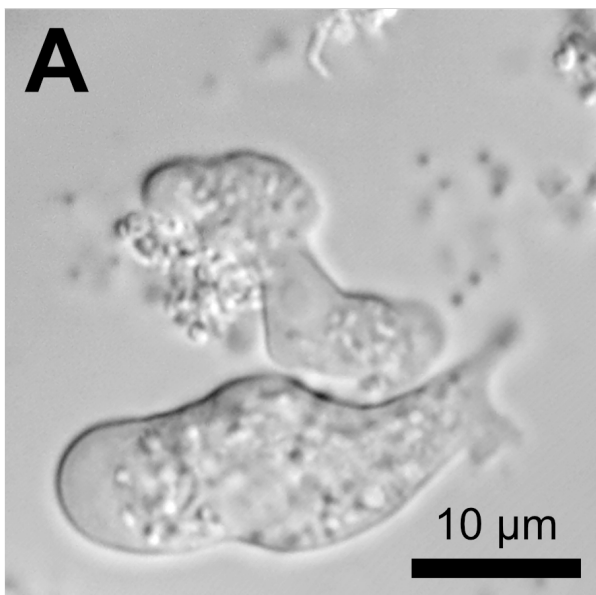
621 **Figure 8:** Light micrographs of *Pharyngomonas* sp. DD1 grazing on *Arthrospira fusiformis*.  
622 Numerous trophozoite cells were observed in the vicinity of cyanobacterial filaments. Large  
623 (A) and smaller (B) vacuoles filled cyanobacterial-derived contents could be observed in the  
624 majority of *Pharyngomonas* sp. DD1 trophozoites. Scale bar is 20  $\mu$ m for both panels.

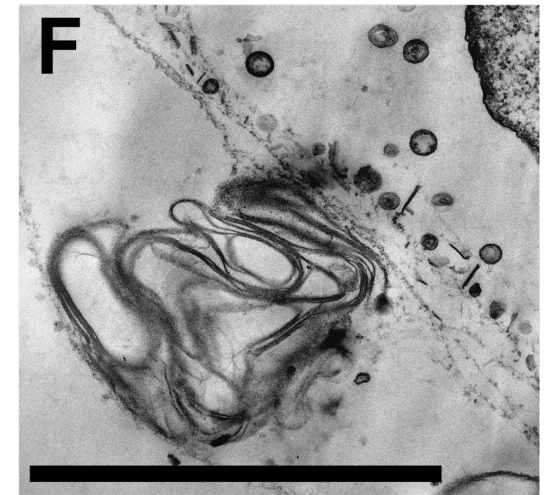
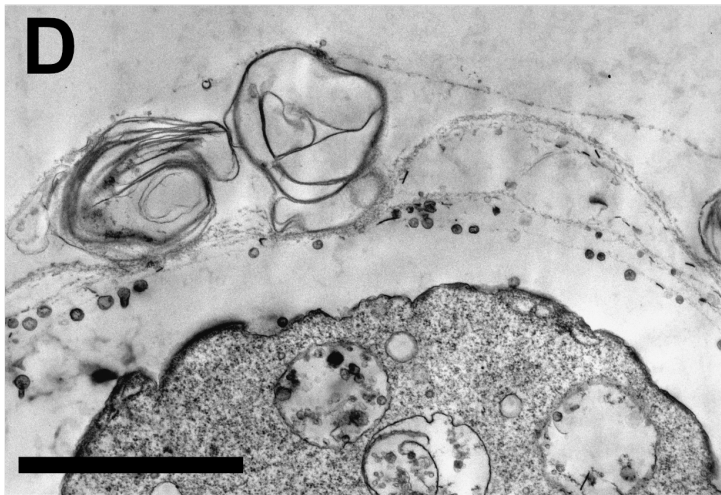
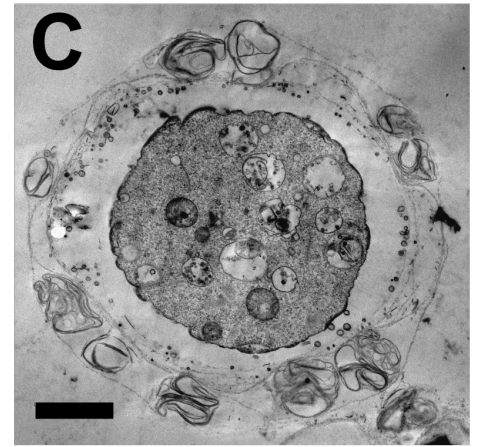
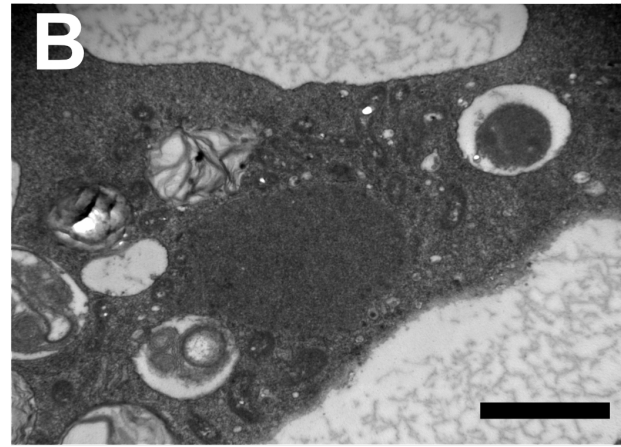
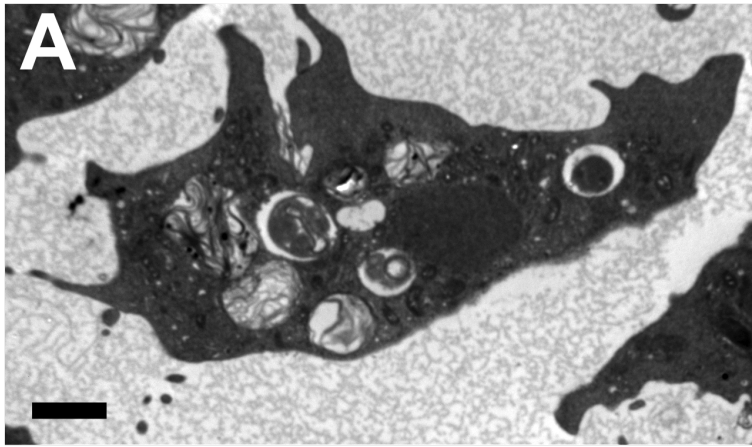
625

# Euglenozoa

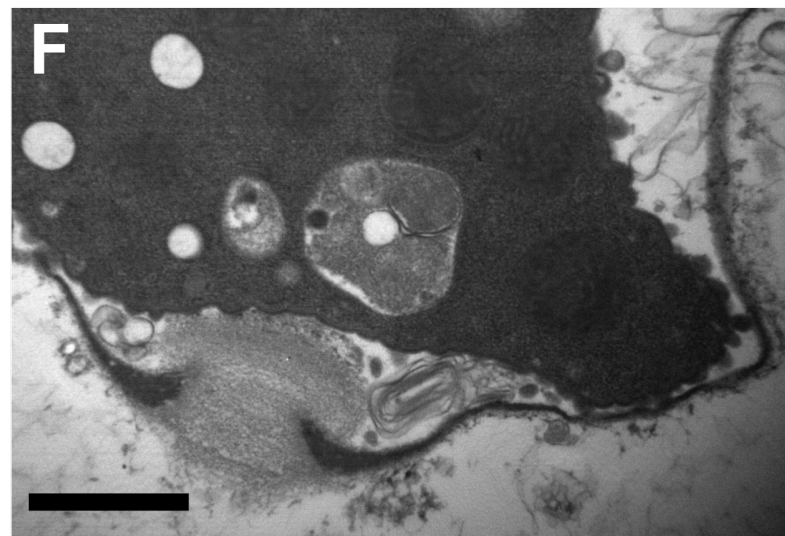
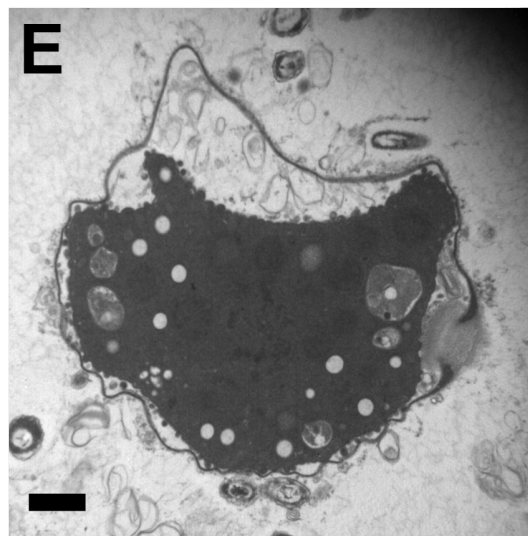
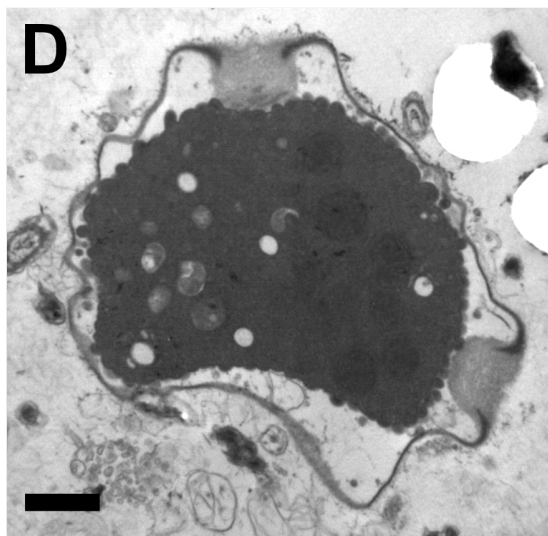
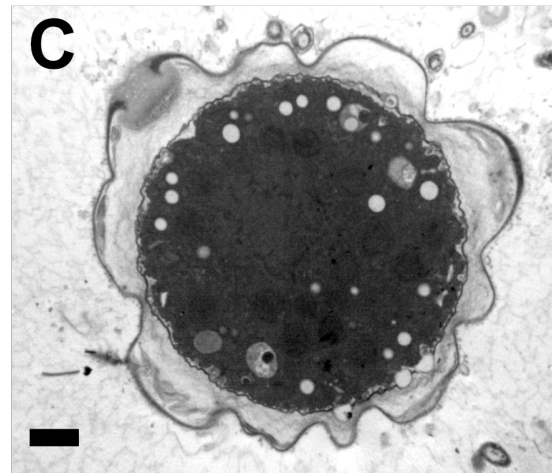
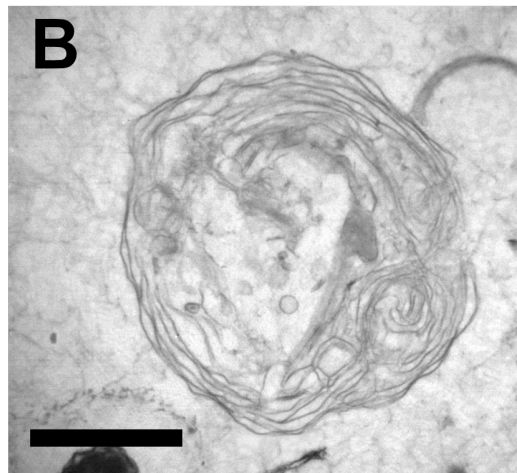
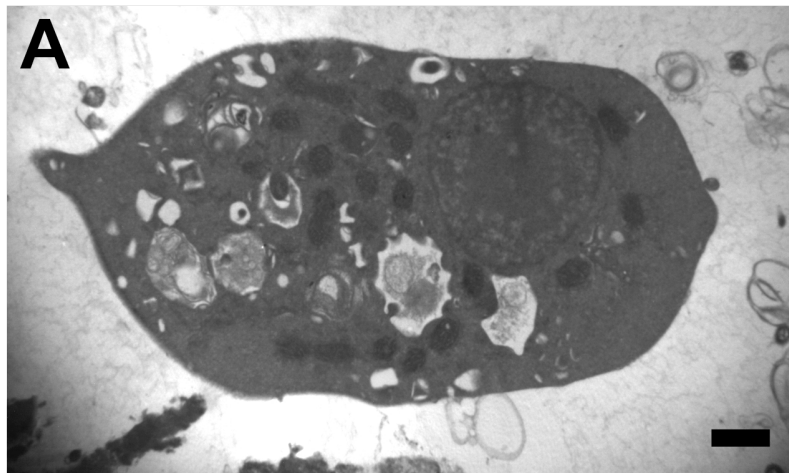




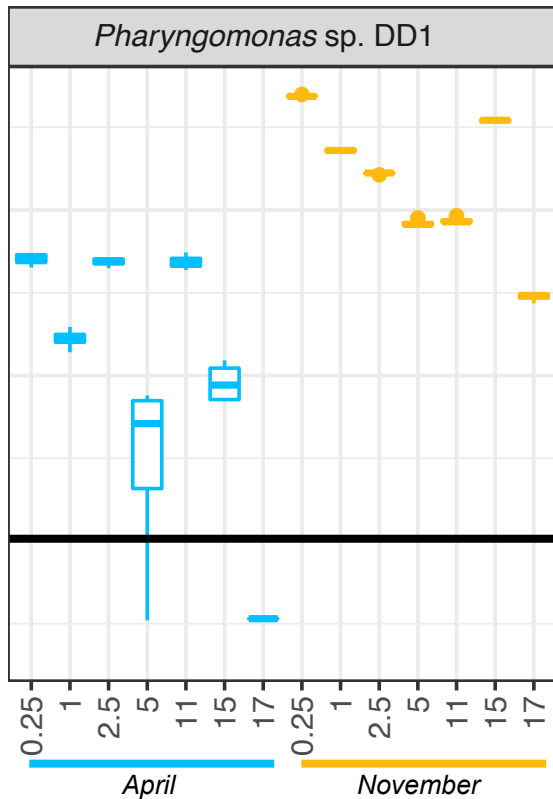
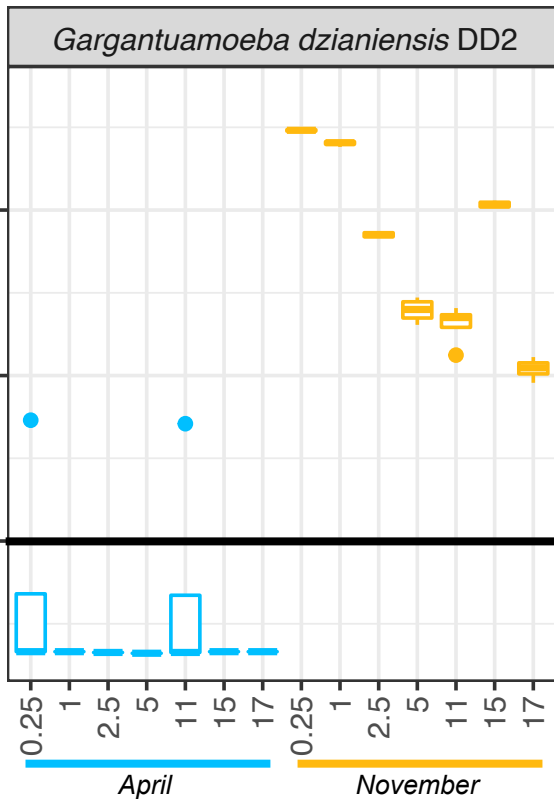








DNA Concentration (ng/mL)



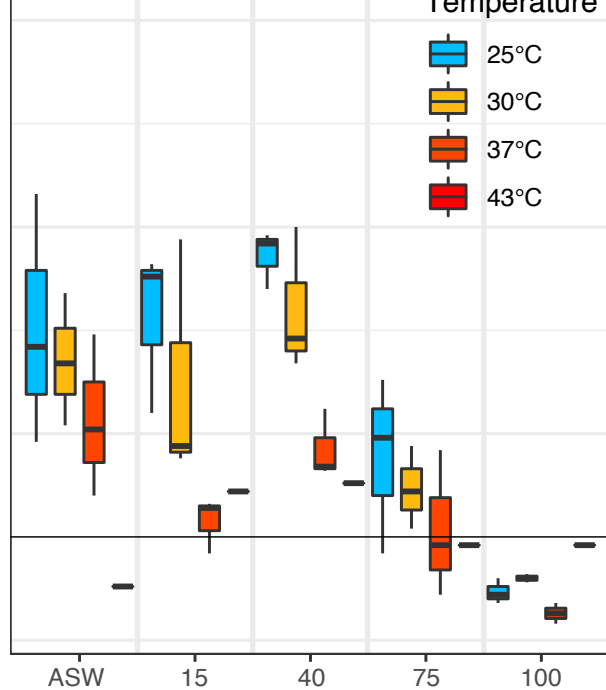
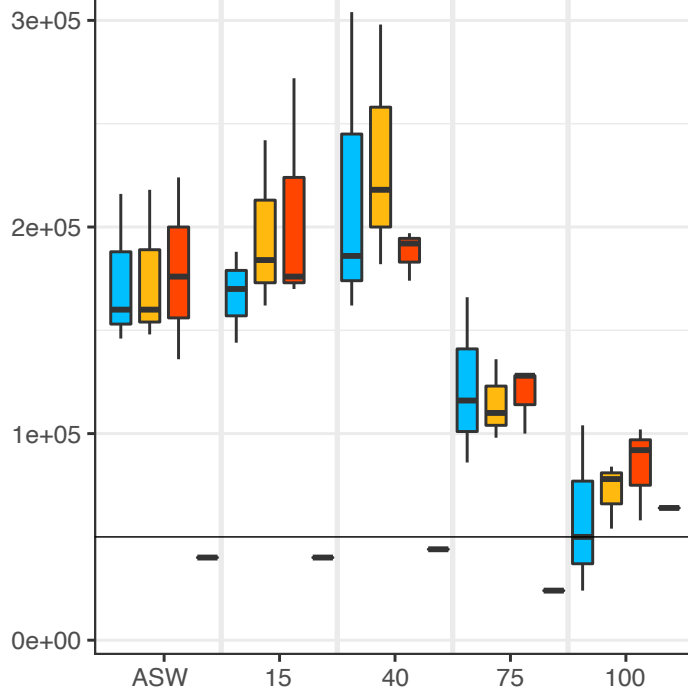
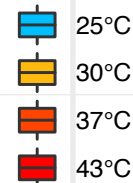
Depth (meters)

Concentration (cells/mL)

*Pharyngomonas* sp. DD1

*Gargantuamoeba dzianiensis* DD2

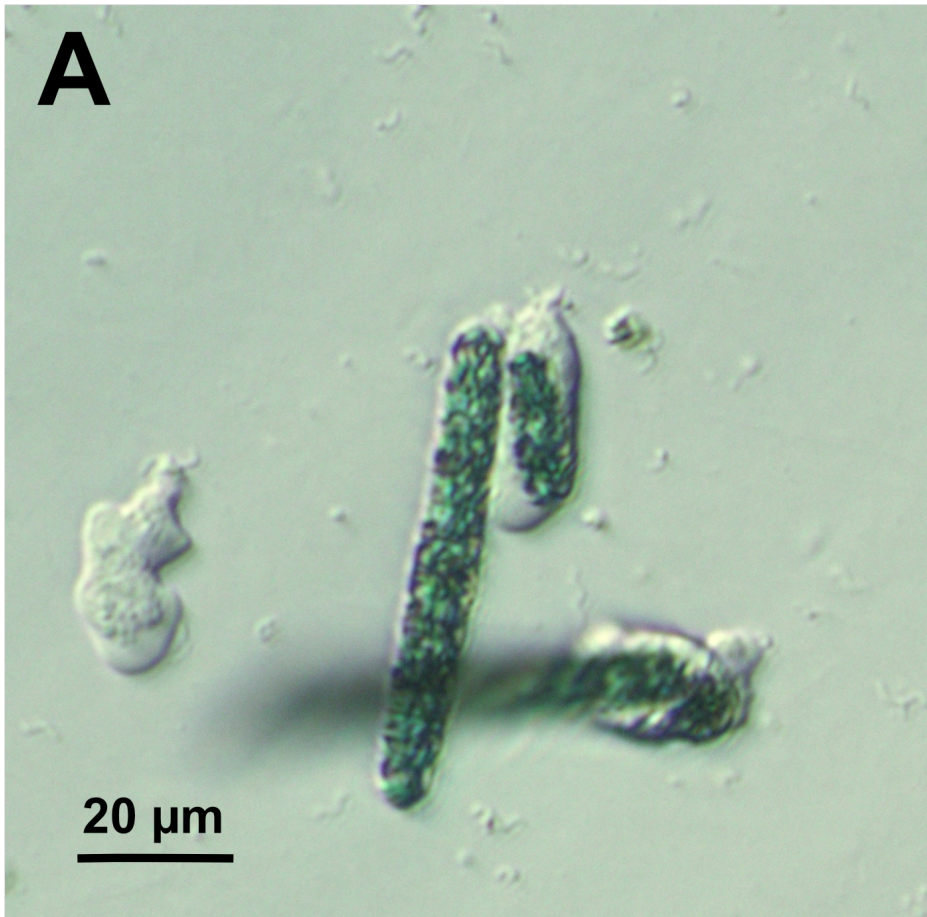
Temperature



Salinity (‰)



**A**



**B**

